Atmospheric Environment Vol. 23, No. 7, pp. 1535–1547, 1989.
Printed in Great Britain.

0004–6981/89 $3.00 + 0.00
Maxwell Pergamon Macmillan plc

COMPOSITION AND ORIGIN OF SUMMERTIME AIR POLLUTANTS AT DEEP CREEK LAKE, MARYLAND

TERI L. VOSSLER*, CHARLES W. LEWIS†, ROBERT K. STEVENS and THOMAS G. DZUBAY
Atmospheric Research and Exposure Assessment Laboratory, U.S. Environmental Protection Agency, Research Triangle Park, NC 27711, U.S.A.

GLEN E. GORDON and SEMRA G. TUNCEL‡
Department of Chemistry, University of Maryland, College Park, MD 20742, U.S.A.

GEORGE M. RUSSWURM
Northrop Services, Inc., Research Triangle Park, NC 27709, U.S.A.

and

GERALD J. KEELER§
Department of Atmospheric and Oceanic Science, University of Michigan, Ann Arbor, MI 48109, U.S.A.

(*First received* 23 *September* 1988 *and in final form* 19 *December* 1988)

Abstract—A 1 month intensive summertime field study conducted in rural western Maryland resulted in a comprehensive set of fine particle, gaseous and meteorological data. Sulfur in the assumed form of ammonium sulfate accounted for 67% of the average fine particle mass and had a very high correlation with fine particle mass ($r = 0.99$). Other measured species, including carbon and nitrate, made only minor contributions to the fine mass. Peak sulfate concentrations, averaged over 6-h intervals, exceeded 50 $\mu g\ m^{-3}$. Nitric acid concentrations showed strong daytime maxima and on a 24 h basis were about four times those of fine particle nitrate. Sulfur in the gas phase (SO_2) constituted more than half of the total sulfur, indicating that the sampling site was being influenced by local sources. Fine particle selenium was well correlated with fine particle sulfur ($r = 0.70$). The ratio of fine particle sulfur to selenium was 2800, characteristic of a rural site downwind of coal-burning areas. Mixed-layer back trajectories were used to identify possible source regions for the measured parameters. Wind frequency-normalized concentrations of parameters associated with coal-burning (S, Se, SO_2 and mass) were highest for back trajectories arriving at Deep Creek Lake from the west-northwest. Use of Rahn and Lowenthal regional signatures showed an overwhelming dominance by the Lower Midwest region, and a surprisingly weak impact by the Upper Midwest region, at the site.

Key word index: Fine particles, sulfur, SO_2, nitric acid and nitrate, mixed-layer back trajectory, regional signatures.

INTRODUCTION

In August of 1983 a comprehensive field study was conducted under the name of the Deep Creek Lake (DCL) field study. The DCL study was part of a larger one involving many participants in which coordinated measurements were performed at three ground level sites, one being near Deep Creek Lake in western Maryland, operated by the EPA, and the others being Laurel Hill and Allegheny Mountain in southwestern Pennsylvania, operated by Ford Research Laboratory (Pierson *et al.*, 1987, 1989). In addition to ground-level ambient measurements, stack sampling was performed at selected local coal-fired power plants and airborne sampling was performed in the power plant plumes. The overall objective of the EPA-supported phase of the field study was to test the feasibility of using regional-scale receptor modeling to determine the impacts of primary and secondary pollutants from coal-fired power plants on ambient air quality. The selection of the DCL site was made with this objective in mind. The DCL site, located on the campus of Garrett Community College in a primarily rural area, was expected to be strongly impacted by coal-fired power plants located within 100 km of the sampling site as well as by coal-burning facilities further to the west in the Ohio Valley region (Fig. 1).

The principal features of the DCL data set are (1) the relatively long duration (1 month) of the study,

*National Research Council Resident Research Associate. Present address: Geophysics Laboratory, Hanscom Air Force Base, MA 01731, U.S.A.
† Author to whom correspondence should be addressed.
‡ Present address: Department of Chemistry, Middle East Technical University, Ankara, Turkey.
§ Present address: Harvard School of Public Health, 665 Huntington Avenue, Boston, MA 02115, U.S.A.

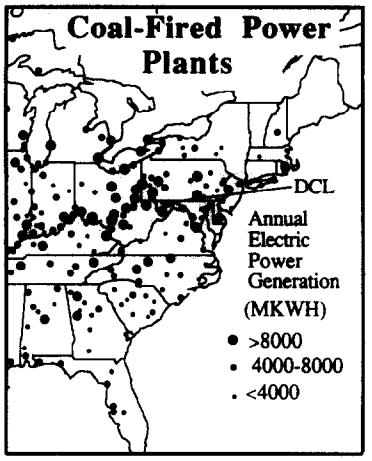

Fig. 1. Coal-fired power plants in eastern U.S.A.

(2) the short time resolution (6-h) of the measurements, (3) the unusually complete chemical characterization of the aerosol and gases, (4) the availability of a complete set of back trajectories with 6-h time resolution, and (5) accompanying measurements of three upwind power plants both in-plume and in-stack. It is the combination of these characteristics that makes the DCL data set unusually attractive.

The present paper serves as an introduction to the ambient results obtained at DCL for fine particles and concurrent gas and meteorological measurements. The overall objective of determining the primary and secondary impact of coal-burning sources using receptor modeling techniques will be addressed in greater detail in papers to follow, as source profile data become available.

EXPERIMENTAL

The data presented in this paper were obtained over the period 1–31 August 1983 at the DCL site (39°34'N, 79°20'W). Particulate samples were collected for four 6-h periods each day beginning at 0400, 1000, 1600 and 2200 EDT. Gaseous species and meteorological parameters were monitored continuously.

Fine and coarse particle samples were collected with a Lawrence Berkeley Laboratory (LBL) dichotomous sampler (Loo *et al.*, 1976) and a Beckman dichotomous sampler having nominal flow rates of 50 and 16.7 ℓ min^{-1}, respectively. Both samplers had a cutpoint of 2.5 μm to separate coarse and fine particles and collect them on 37-mm dia. 2-μm pore size Teflon filters. Although both coarse and fine particle samples were available, only the fine particle data are presented here. Analyses by β-ray attenuation for mass (Courtney *et al.*, 1982) and by X-ray fluorescence (XRF) for elemental composition (Dzubay *et al.*, 1982) were performed at the Atmospheric Research and Exposure Assessment Laboratory on filters collected with the LBL sampler. Instrumental neutron activation analysis (INAA) was performed at the National Bureau of Standards (NBS) research reactor. Only one-third of the INAA samples were from the LBL sampler, with the remainder from the Beckman sampler.

Species measured continuously were SO_2, O_3, NO, NO_2 and NO_x, as well as light scattering, temperature, dewpoint and solar insolation. Sulfur dioxide was measured with a TECO model 43 pulsed u.v. fluorescence analyzer with a rated accuracy the larger of 2 ppb or 10%; O_3 was measured with a Bendix model 8002 chemiluminescence analyzer with a rated accuracy the larger of 1 ppb or 10%; NO, NO_2 and NO_x were measured with a Bendix model 8101-B chemiluminescence analyzer with a rated accuracy the larger of 5 ppb or 10%. Accuracies for the gas monitoring devices were verified by three multipoint calibrations performed over the course of the study. Zero and span calibrations were made at least every other day. Light scattering, represented by bsph, was monitored with an MRI model 1561 integrating nephelometer with 10% accuracy. Air passing through the nephelometer was heated approximately 10°C to reduce relative humidity effects. The instrument was calibrated with Freon-12 three times during the study, and precision checks were performed twice daily. Temperature and dew point were monitored with a Climatronics sensor model 100325-2 with ± 2°C accuracy. Solar insolation was monitored with an Eppley pyranometer model 2; an accuracy $< 5\%$ was inferred from comparisons of the device with standards performed at NBS over the preceding several years. Continuously monitored data were first averaged over 1-h intervals, deleting 1-h intervals which included calibrations. The remaining 1-h data were then averaged over the 6-h intervals corresponding to the sampling schedule of the dichotomous samplers.

The denuder difference method (Shaw *et al.*, 1982) was employed to measure separately nitric acid and particulate nitrate. Ambient air passed through a Teflon cyclone at about 30 ℓ min^{-1} to remove particles larger than 2.5 μm. Portions of the airstream subsequently passed through parallel denuding and non-denuding legs and finally to the corresponding nylon filters (Membrana 1-μm pore size). Flow through each leg was limited to about 3 ℓ min^{-1} by critical orifices. The daily sampling schedule for the denuder difference apparatus included one 6-h daytime sample starting at 1000 EDT and one 18-h sample starting at 1600 EDT. The denuder difference nylon filter samples were extracted and analyzed for nitrate by ion chromatography at EPA by Northrop Services, Inc.

Fine particle samples for carbon analysis were collected on quartz filters (Pallflex type 2500 QAST) with a modified Sierra dichotomous sampler (Stevens, 1986) at an average flow rate of 26 ± 1 ℓ min^{-1}. These samples were sent to Sunset Laboratory in Forest Grove, Oregon for the analysis of elemental carbon (CEL) and volatilizable carbon (CVOL) by a thermal–optical method, similar to that of Johnson *et al.* (1981).

RESULTS AND DISCUSSION

Diurnal averages

Parameter averages at DCL are presented in Table 1. Averages are given for all samples as well as for daytime (1000–2200 EDT) and night-time (2200–1000 EDT) sampling intervals. In general only those parameters with average uncertainties $\leqslant 30\%$ were included in this summary. Exceptions were NO, NO_2 and NO_x, which were measured near their detection limits. Usually the uncertainty given in the last column is the average standard deviation for a single measurement divided by the 'all cases' mean. For the calculated ratios S/Se and S_g/S_p, however, the uncertainty is the coefficient of variation for 'all cases'. Most of the averages are based on a common set of 98 cases having no missing values, out of 120 possible cases. The carbon averages (CEL and CVOL) are based on 97 cases, but about 20% of the cases are not

Table 1. Fine particle, gas and meteorological parameter averages measured at Deep Creek Lake during August 1983

			All		Day		Night		
Parameter*	Method	Units	No. cases	Mean	No. cases	Mean	No. cases	Mean	Uncertainty
Mass	BETA	ng m^{-3}	98	40,000	51	47,000	47	32,000	7%
CEL	THERM	ng m^{-3}	97	180	51	160	46	190	24%
CVOL	THERM	ng m^{-3}	97	1450	51	1390	46	1520	7%
NO_3^-	DDM	ng m^{-3}	59	570	29	650	30	500	20%
HNO_3	DDM	ng m^{-3}	59	2500	29	4100	30	1100	30%
Na	INAA	ng m^{-3}	98	34	51	36	47	33	19%
Si	XRF	ng m^{-3}	98	150	51	170	47	130	23%
S	XRF	ng m^{-3}	98	6700	51	7800	47	5500	9%
K	XRF	ng m^{-3}	98	44	51	46	47	42	11%
Ca	XRF	ng m^{-3}	98	48	51	57	47	39	11%
Sc	INAA	ng m^{-3}	98	0.013	51	0.015	47	0.010	23%
V	INAA	ng m^{-3}	98	0.81	51	0.91	47	0.71	11%
Mn	INAA	ng m^{-3}	98	3.2	51	3.2	47	3.1	8%
Fe	XRF	ng m^{-3}	98	58	51	60	47	55	9%
Zn	XRF	ng m^{-3}	98	13	51	12	47	13	12%
As	INAA	ng m^{-3}	98	0.80	51	0.79	47	0.80	9%
Se	INAA	ng m^{-3}	98	2.5	51	2.5	47	2.5	7%
Br	XRF	ng m^{-3}	98	5.3	51	4.8	47	5.9	14%
Sb	INAA	ng m^{-3}	98	0.66	51	0.50	47	0.83	17%
La	INAA	ng m^{-3}	98	0.08	51	0.09	47	0.07	23%
Pb	XRF	ng m^{-3}	98	48	51	46	47	50	9%
SO_2	CONT	ppb	98	8	51	10	47	5	2 ppb
NO_x	CONT	ppb	98	5.1	51	4.0	47	6.4	5 ppb
NO	CONT	ppb	98	1.2	51	0.3	47	2.1	5 ppb
NO_2	CONT	ppb	98	4.0	51	3.8	47	4.3	5 ppb
O_3	CONT	ppb	84	48	44	61	40	34	10%
bsph	CONT	m^{-1} 10^4	98	1.2	51	1.4	47	1.0	10%
SRAD	CONT	W m^{-2}	98	260	51	410	47	90	5%
WSPD	TRAJ	km h^{-1}	93	18	49	18	44	18	25%
RHUM	CALC	%	97	64	51	57	46	72	10%
TEMP	CONT	°C	98	19	51	22	47	16	2°C
S/Se	CALC	None	97	2800	51	3400	46	2100	54%
S_g/S_p	CALC	None	98	1.5	51	1.5	47	1.4	88%

* Mass = fine particle mass; CEL = elemental carbon; CVOL = volatilizable carbon; NO_3^- = particulate nitrate; bsph = light scattering coefficient from heated nephelometer; SRAD = solar radiation; WSPD = wind speed; RHUM = relative humidity; TEMP = temperature; S_g = gaseous sulfur; S_p = S = particulate sulfur.

XRF = X-ray fluorescence; INAA = instrumental neutron activation analysis; BETA = β-gauge method; THERM = thermal–optical technique; CONT = continuous monitoring instrument; DDM = denuder difference method; TRAJ = mixed-layer back trajectories; CALC = calculated from above data.

Day is 1000–2200 EDT.

Night is 2200–1000 EDT.

common to the 98 case set. The number of cases shown for HNO_3 and NO_3^- is deceptive as only two samples per day were available, one being an 18-h sample.

Table 1 shows that S was the dominant fine particulate species and, when expressed as SO_4^{2-} ion, constituted 49% of the average fine particle mass. The percentage increases to 67% if the S were in the form of $(NH_4)_2SO_4$ at the time of analysis, which was likely the case since no precautions were taken to preserve the acidity of the original sample. Both S and SO_2 were higher during the day than at night.

The Br/Pb ratio, typically found in the range 0.3–0.4 in urban areas (Lewis *et al.*, 1987; Koutrakis and Spengler, 1987), consistent with a motor vehicle origin, was 0.11 for all DCL samples. Since the Pb–Br correlation coefficient was 0.80, a predominantly motor vehicle origin is still likely, but the low Br/Pb ratio found at DCL is indicative of an acidic aerosol, which can displace bromine. In fact electron microscopic measurements (Mamane and Dzubay, 1986) on DCL aerosol samples showed a large contribution from acidic sulfates. In addition high aerosol acidities were frequently measured concurrently at the two sites operated by Ford Research Laboratory (Pierson *et al.*, 1989).

The ratios of gaseous to particulate nitrate, HNO_3/NO_3^-, were about 6:1 for the 6-h daytime periods and 2:1 for the 18-h 'night-time' periods. Samples confined strictly to hours of darkness presumably would have shown an even smaller HNO_3/NO_3^- ratio. Table 1 shows that particulate NO_3^- concentrations were rather constant, so that most of the diurnal variation in the ratio is due to HNO_3 changes. Such a diurnal variation of HNO_3 is

consistent with photochemical formation of its precursors during daytime and rapid depletion, largely by dry deposition, during night-time.

CEL and CVOL together constituted a small fraction of the total fine particle mass, averaging only 4%. The percentage would increase to no more than 5% if the H and O associated with CVOL were included (Countess *et al.*, 1980; Shah *et al.*, 1984). Particulate NO_3^- and its associated cation (probably NH_4^+) was the next most important contributor to fine particle mass, yet accounted for only 2% of the fine particle mass. All other measured fine particle species were negligible contributors.

The average S/Se ratio was 2800 ± 1500 (mean $\pm$ std dev) for all samples. This agrees with the 3000 ratio found by Tuncel *et al.* (1985) for rural sites well downwind of coal-burning areas. The average ratio of gaseous to particulate sulfur, S_g/S_p, shows more than half of the total sulfur (as S) was present in the gaseous state, indicating the presence of local sources.

Analysis of samples by INAA provided concentrations of many elements in addition to those measured by XRF. Particular elements that are measured reasonably well by either method provide a means of quality assurance for the two methods. Ratios of concentrations of five such elements measured for the same sampling intervals by XRF and INAA are presented in Table 2. Even though most XRF and INAA samples were not physically the same filter, the ratios are generally consistent with unity within their uncertainties. The best agreements are for Fe and Zn, which also have the smallest uncertainties. For each element either the XRF or INAA measurement results were chosen according to which method had the smaller analytical error. It should be remembered that the XRF samples were on average more heavily loaded and thus analytically more favorable, since they were obtained at 50 ℓ min^{-1}, while two-thirds of the INAA samples were from 16.7 ℓ min^{-1} sampling.

Temporal variations of key parameters

Figure 2 shows the temporal variation of some closely associated species. Fine particle concentrations of mass (Fig. 2a) and S (Fig. 2b) tracked each other remarkably well. This is a consequence of the fact that up to 67% of the fine particle mass was SO_4^{2-} and related cations, as detailed above. The remarkable similarity of these two parameters also serves an important quality assurance role since the underlying analytical procedures (β-ray attenuation and XRF) are quite different. Selenium, thought to be a possible tracer for coal-fired power plants, tracked S fairly well (Fig. 2c). For contrast Pb was also included in this comparison since it is a common well-measured element, but is not expected to dominate fine particles or behave the same as elements whose primary source is coal combustion. Indeed, the Pb variation (Fig. 2d) has very little similarity to the others. A striking feature of these figures is the very high concentrations (e.g. >50 μg m^{-3} for S expressed as SO_4^{2-}) attained during peak periods, which is emphasized by the short sampling periods.

Table 2. Ratios of XRF/INAA concentrations for the DCL fine particle samples

Parameter	No. cases	Ratio of means XRF/INAA
S	98	1.34 ± 0.31
Fe	98	0.87 ± 0.18
Zn	98	0.98 ± 0.18
Se	106	1.32 ± 0.24
Br	98	1.33 ± 0.41

Wind directional dependence of parameters

The behavior of measured and calculated parameters with respect to wind direction was examined with mixed-layer back trajectories calculated using the ARL-ATAD model (Heffter, 1980). The trajectories represent the most probable path of an air parcel advected with the mixed layer-averaged winds. A back trajectory is useful for establishing the *direction* of arrival of a pollutant species, but does not of itself give any information on the *distance* to the source in that direction. Trajectories were calculated by the method of Samson (1980) starting at the sampling site and moving backwards in time in 3-h increments using available National Weather Service upper-air observations. Mixed-layer trajectories such as that shown in Fig. 3 were calculated for air arriving at DCL at 0200, 0800, 1400 and 2000 EDT, roughly corresponding to the midpoints of the sampling periods, for the entire study. With DCL at the center, the area was divided into eight equal sectors as shown in Fig. 4. Using the last 24 h of each trajectory the average wind sector frequency distribution, $[F_j]$, was calculated via

$$[F_j] = \sum P_{ij}/N \quad (1)$$

where P_{ij} is the fraction of the 24-h trajectory lying in wind sector j for sampling period i, and N is the number of sampling periods. The results of Equation (1) are shown in the first line of Table 3. Three of the wind sectors (ESE, SSE and SSW) occurred with insignificant ($<3\%$) frequency and were not included in the table.

The choice of 24 h represented a compromise between the desirability of identifying potential sources as distant as possible and the increasing lack of definition of an extended trajectory. Twenty four hours was also a practical choice since it was the longest duration for which back trajectories were available for virtually every sampling period. For an average wind speed of 18 km h^{-1} (Table 1), 24 h is equivalent to more than 400 km.

The average fractional contribution to parameter k from each wind sector j is also given in Table 3, as

calculated from

$$[C_{kj}]/[C_k] = \frac{1}{N}\sum(C_{ik} * P_{ij})/[C_k]. \quad (2)$$

For an alternative comparison, the mean values of each parameter in each wind sector were normalized with respect to wind sector frequency, as given by

$$\text{normalized } [C_{kj}] = [C_{kj}]/[F_j]. \quad (3)$$

The normalization step insures that there is no bias toward any wind sector because of its frequency of occurrence. In other words, the calculation gives the average concentrations seen when the wind is only from the indicated wind sector, effectively a 'wind sector source profile'. This procedure is similar to that used by Parekh and Husain (1982).

Wind frequency-normalized values of important parameters are plotted in Fig. 5 for each of the five important wind sectors. Parameters have been grouped together if the highest normalized concentration for each occurs in the same wind sector. For example Sc, V and As are grouped because their

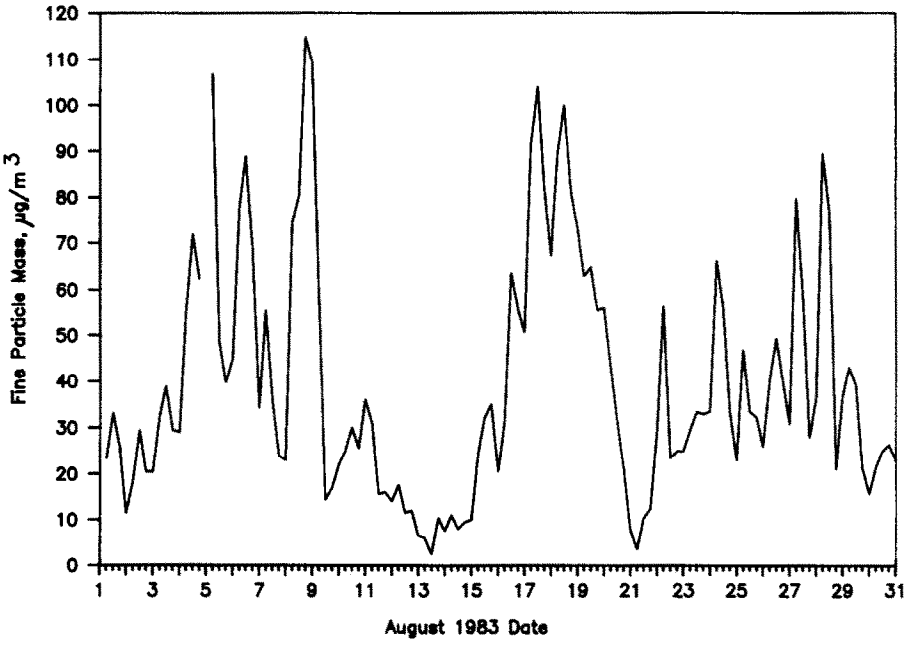

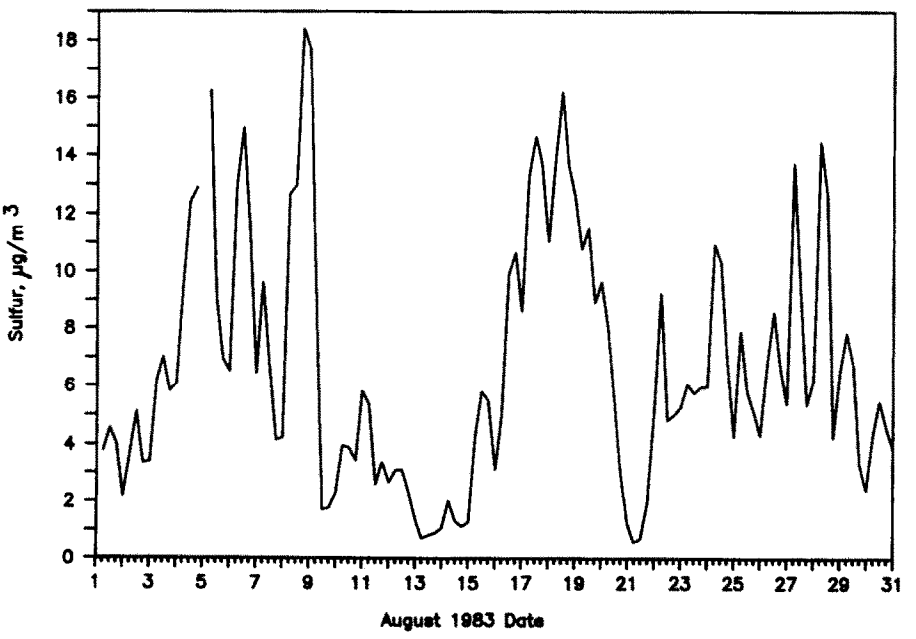

Fig. 2(a,b).

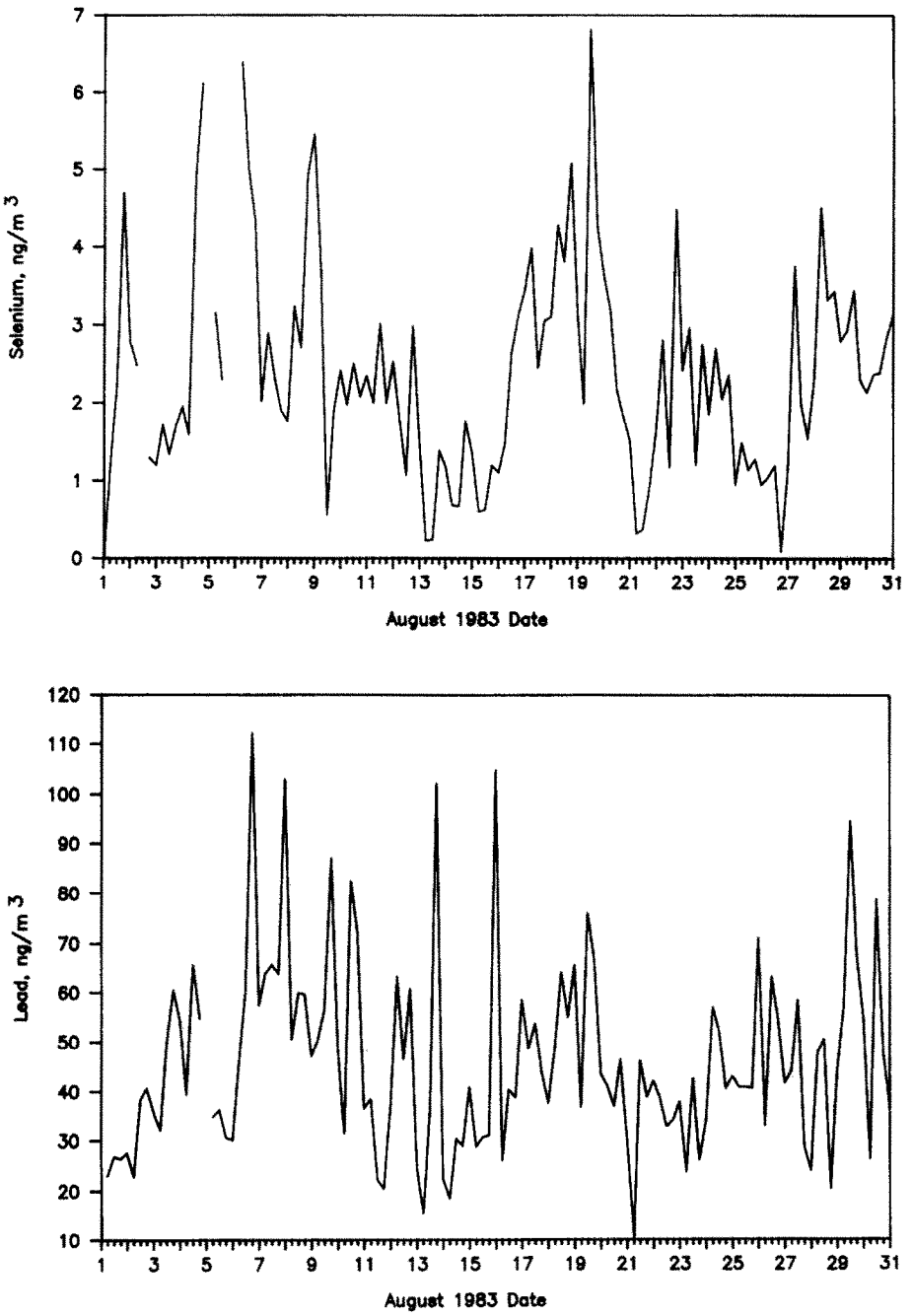

Fig. 2. Concentrations of (a) fine particle mass, (b) sulfur, (c) selenium and (d) lead as functions of the sampling interval indicated by each tick mark on the x-axis.

highest concentrations all occur in the ENE sector. The association of high V loadings with ENE is expected, because of the dominance of oil-burning power plants in the eastern and northeastern U.S.

Less expected were the higher concentrations of soil-related elements (Ca, Fe and Si) associated with the WSW sector. Tuncel *et al.* (1985) also observed that the concentrations of Al and Si at the EPA Shenandoah Valley sampling site (130 km south-southeast of DCL) were highest for southwest trajectories.

Normalized values of parameters associated with coal-burning power plants (S, Se, SO_2, mass and bsph) were highest for WNW trajectories. Figure 1 clearly shows the greatest concentration of coal-fired power plants to be in the NNW–WNW–WSW directions. The ratio S_g/S_p is largest for the WNW and NNW wind sectors, indicating a greater relative impact of local vs distant SO_2 sources in the northwest quadrant.

Normalized concentrations of elements related to other anthropogenic activity (Mn, Zn, Br and Pb)

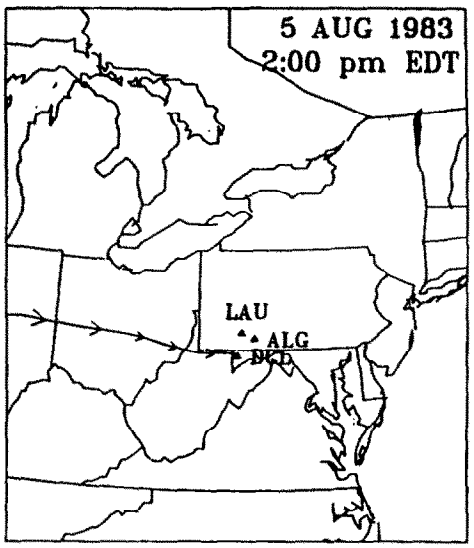

Fig. 3. Mixed-layer back trajectory example. Sampling sites at Deep Creek Lake (DCL), Allegheny Mountain (ALG) and Laurel Hill (LAU) are shown.

Table 3. Per cent contribution to average parameter value for five wind sectors

Parameter	ENE	NNE	NNW	WNW	WSW
Wind frequency	6	16	29	28	21
Mass	4	7	28	37	24
CEL	6	12	28	26	24
CVOL	5	11	30	30	21
NO_3^-	5	11	28	27	25
HNO_3	5	8	36	28	20
Na	7	14	25	30	24
Si	3	13	26	32	27
S	4	7	28	38	24
K	4	12	31	31	22
Ca	5	16	26	28	25
Sc	9	14	27	28	23
V	10	25	26	23	16
Mn	2	12	38	31	17
Fe	3	11	34	30	22
Zn	3	9	42	29	17
As	9	17	40	22	13
Se	3	10	32	34	21
Br	4	16	30	27	22
Sb	5	10	30	29	27
La	3	11	21	34	31
Pb	4	14	34	28	20
SO_2	3	6	31	43	17
bsph	3	7	28	38	24

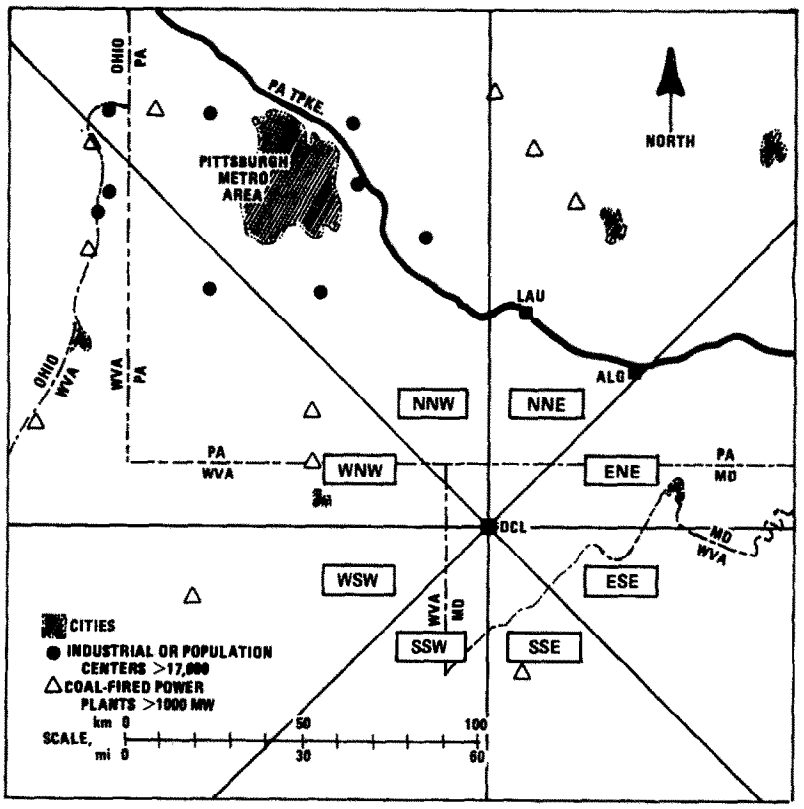

Fig. 4. Wind sector identification.

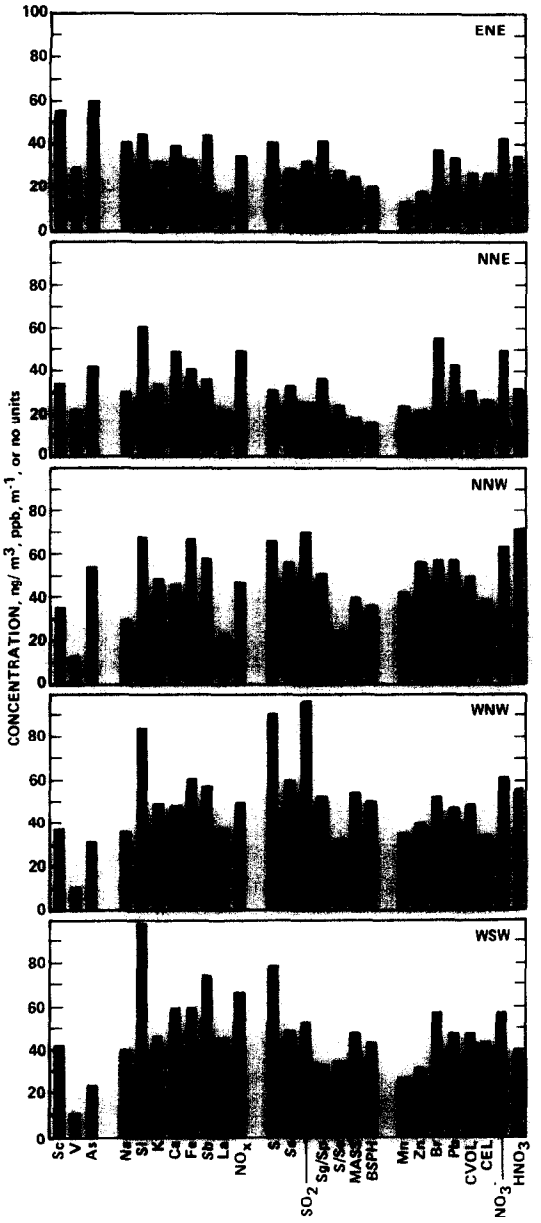

Fig. 5. Average wind frequency-normalized concentrations of parameters for five wind sectors observed at DCL. Concentrations were multiplied by the following scale factors: Sc (3000), V (20), As (50), Na (1), Si (0.5), K (1), Ca (1), Fe (1), Sb (100), La (400), NO_x (10), S (0.01), Se (20), SO_2 (8), S_g/S_p (30), S/Se (0.01), MASS (0.001), BSPH (30), Mn (10), Zn (3), Br (10), Pb (1), CVOL (0.03), CEL (0.2), NO_3^- (0.1) and HNO_3 (0.02).

were highest for the NNW direction. Pittsburgh, PA, is located 110 km NNW of DCL and is most likely the dominant source area for those elements (Fig. 4).

Regional signature comparison

Rahn and Lowenthal (1985) have developed a regional tracer system in which they characterize air masses from five regions of North America by the ratios of concentrations of six tracer elements to that of Se. They assume the air is sufficiently well mixed within the regions, having dimensions of hundreds of kilometers, and the ranges for the ratios are narrow enough, that particles in the air emerging from each region can be identified by their trace element concentrations. In most areas the major portions of the six elements (V, Mn, Zn, As, In and Sb) and Se are contributed by anthropogenic air pollution sources. However substantial amounts of V and Mn are contributed by soil and other crustal materials, so Rahn and Lowenthal (RL) use 'non-crustal' portions of them, obtained by subtracting crustal contributions calculated from Al concentrations in each sample multiplied by the (V/Al) and (Mn/Al) ratios of Mason's crustal abundance pattern (1966). As RL work mainly with Hi-vol samples, which include particles up to 30 μm dia. or more, their crustal corrections are often quite large.

To compare our results with the RL model, one cannot simply sort the samples according to back trajectory and see if the ratios vary as expected based on the origin of the air mass: as the DCL site is near the upper end of RL's Lower Midwest (LMW) region, most samples are expected to contain an LMW contribution, with perhaps contributions from other regions more distant on the trajectory. In fact RL obtained their LMW signature from measurements made at the Allegheny site (Fig. 4) during part of the same August 1983 period the DCL measurements were being made. Therefore instead we performed chemical mass balances (CMBs) to fit the observed concentrations of the seven elements (including Se) of each sample by a linear combination of RLs signatures for each of the five regions. For V and Mn non-crustal portions of these elements in each ambient sample, calculated by RLs procedure, were used. As anticipated the crustal corrections were small, because of the fine particle nature of the samples. Even though In was poorly measured this element was included in the CMBs because of its importance in identifying the presence of the Southern Ontario (SONT) signature. Indium concentrations above the analytical detection limit (0.003 ng m^{-3}) were measured for about a third of the samples. For the rest a constant value of half the detection limit was assumed, effectively defining a non-zero upper limit for the SONT contribution.

In the CMB procedure the concentration of element i is given by:

$$C_i = \sum_{j=1}^{5} m_j x_{ij}, \tag{4}$$

where x_{ij} is the concentration of element i in particles from region j, and m_j is the strength of the signature from region j in the sample, i.e. the 'regional coefficient' (because the signatures are normalized to Se = 1.00, m_j is the concentration of Se contributed from region j). The m_j values for each sample were obtained from an effective-variance least-squares fit, which

Table 4. Average regional coefficients of Rahn and Lowenthal tracer system vs wind sector of back trajectory

Wind sect.	No. cases*	Regional coefficients† NENG	CEC	LMW	UMW	SONT
WSW	23.1	<0.001	0.01±0.03	1.90±0.84	0.02±0.06	<0.003
WNW	27.5	0	0.01±0.03	2.41±0.94	0.04±0.11	<0.002
NNW	27.0	<0.002	0.005±0.018	2.23±1.10	0.31±0.40	0.005±0.015
NNE	15.1	0.004±0.019	0.023±0.022	1.21±0.93	0.17±0.22	0.007±0.007
ENE	5.2	0	0.11±0.14	1.00±0.81	0.15±0.13	0.008±0.006

* Non-integer because trajectories for many sampling periods were apportioned to more than one sector.
† Uncertainties are standard deviations of the coefficients for events falling within the sector.

takes account of the errors in both the observed concentrations and the regional signatures (Watson *et al.*, 1984).

Results of the CMBs are summarized in Table 4, which lists the average regional coefficients for the 98 samples for which there were no missing values of Se or Al or any two other elements. As was done above, samples were assigned proportionally to more than one wind sector if the back-trajectory was not confined to a single sector, thus accounting for the non-integral number of cases falling within each sector.

The LMW signature was present in all 98 samples, in 20 of them being the only non-negative contribution. Forty-seven samples had contributions from LMW and one other region, 14 from two other regions, 16 from three and only one sample had non-negative strengths from all five regions. The CMBs involving regional signatures are different from those of an urban area, in which a half dozen or so source signatures are typically resolved from each sample's composition pattern. Rahn and Lowenthal (1985) indicated that most samples collected at Underhill, VT, and Narragansett, RI, have contributions from only one or two regions.

As expected, the LMW signature is the only significant contributor for back trajectories from the WSW. It is also strongly dominant for WNW. In part, this dominance may arise from the fact that coal-fired power plants of the Ohio River Valley are very strong sources in the LMW, so its signature is probably that of distant coal-fired plants with small contributions from other sources in that region. Thus, the many coal-fired plants in the WNW sector probably contribute particles at DCL whose trace element signature is dominant in all sectors, but with lower absolute strengths in the easterly sectors, where there is less coal combustion.

The Upper Midwest (UMW) signature is supposed to be associated with the lower Great Lakes region, including Chicago, Cleveland, Detroit, etc., which release particles from metals and manufacturing processes, as well as from coal combustion, motor vehicles, etc. The UMW signature is richer than LMW in all of the tracer species relative to Se, by ratios ranging from 4.5 to 6.5, except for Sb, for which it is richer by a facto of 2.9. The major surprise in Table 4 is the weakness of the UMW regional coefficient for the WNW sector, where it should be strongest. The UMW strength is somewhat greater in the NNW sector, but still far from dominant, and it is stronger in the easterly sectors than in WNW! Altogether there is very little evidence for a UMW impact at the DCL site.

As expected, higher ncr-V/Se ratios in samples associated with the ENE sector yield detectable contributions of the Central East Coast (CEC) signature, a region characterized by oil combustion. The New England (NENG) and Southern Ontario (SONT) coefficients are always quite small.

After determining the regional coefficients for each sample, RL apportion sulfate by first performing a regression of its concentration vs the regional coefficients. We performed a multiple linear regression of the S concentrations vs the regional coefficients, obtaining only two significant, non-negative terms:

$$S(\text{ng m}^{-3}) = (3190 \pm 160)[m_{\text{LMW}}] + (12{,}400 \pm 7300)[m_{\text{CEC}}],\ r^2 = 0.39 \quad (5)$$

where the coefficients, 3190 and 12,400, are the S/Se ratios of particles from the LMW and CEC regions. Lowenthal and Rahn (1988) obtained corresponding ratios (after scaling SO_4^{2-} to S) for LMW of 2400 and 3500 for samples collected at Narragansett and Underhill, respectively, which bracket our value of 3190. As Tuncel *et al.* (1985) have noted, values of about 3000 are observed far from the sources, where much of the SO_2 has converted to SO_4^{2-}, but values around 1700 are more typical of areas near coal-fired plants, where most of the Se, but little of the S from nearby sources, is borne by particles. Thus, we are surprised to find S/Se ratios for LMW at DCL as high as those observed much farther away by RL.

The S/Se ratios for CEC particles observed at Narragansett and Underhill (Lowenthal and Rahn, 1988) are 2500 and 7000, respectively, vs our value of 12,400. In this case, their samples are taken close to the region and ours more distant, so we expect to see a higher ratio, but its uncertainty is so large that one cannot draw strong conclusions.

Inserting the average m_{LMW} and m_{CEC} values in Equation (5), we find that the average S concentrations contributed by the LMW and CEC regions at the DCL site are 6.3 and 0.4 μg m^{-3}, respectively.

Linear correlations

Table 5 shows linear correlation coefficients of many of the species from Table 1. For 95 observations, a correlation greater than 0.26 is significant at the 1% confidence level. Any correlations below this value are omitted. The reduced number of cases compared with those used in Table 1 came from the decision to eliminate apparent outliers, arbitrarily defined as a parameter value different from its mean by at least a factor of ten. Thus a single case each for V and Sb was omitted. The omissions strongly affected eleven of the correlation coefficients associated with Sb (in all cases increasing them from the 0.07–0.17 range to the 0.28–0.44 range) and three associated with V (V–NNE increased from 0.11 to 0.40, while V–Sc decreased from 0.47 to 0 and V–ENE decreased from 0.58 to 0.40). The outlier cases were retained in Table 1 (but not in any of the other calculations in this article) since their effect on the means was generally within the uncertainties given in Table 1.

Table 5 is arranged so that parameters with mutually high correlations tend to occur as clusters near the diagonal. While a high correlation between two elements does not necessarily indicate a common source, we nevertheless feel that careful examination of a correlation table is a useful diagnostic exercise, comparable to that of a factor analysis.

Proceeding down the diagonal the highest correlations occur among SO_2, Se, S and fine mass, which are all related to coal-fired power plant emissions. The WNW wind sector is the only one that is correlated (weakly) with these elements. Figure 1 supports the WNW as a general source area for coal-fired power plant emissions. The extremely high correlation of S with fine mass ($r = 0.99$) is consistent with the earlier observation that S, if present in the form of ammonium sulfate at the time of laboratory analysis, accounts for 67% of the fine particle mass. Since it was noted that the other major particulate species (organics and nitrates) can account for no more than an additional 7% of the fine mass, the extremely high correlation coefficient suggests that most of the mass which is not accounted for is likely to be water of hydration associated with particulate sulfate.

The substantial correlation of S and Se (0.70) is similar to that observed concurrently at the Allegheny Mountain and Laurel Hill sites for these elements in the fine fraction, 0.75 and 0.71, respectively, for about forty cases at each site (Pierson, pers. comm., 1988). The histogram (not shown) of the DCL S/Se ratios was essentially unimodal, with a mean and standard deviation of 2800 ± 1500, as indicated above.

Unexpected are the substantial (for 95 cases) correlations of Si with S and fine mass (0.61 and 0.66), and its moderate correlations with SO_2 and Se (0.45 and 0.42). Similar sized fine particle correlations of Si with SO_4^{2-}, mass, SO_2 and Se (approximately 0.60 for about 40 cases) were also found at each of the two Ford Research Laboratory sites operated concurrently with the DCL site (Pierson, pers. comm., 1988). We speculate that the origin of the Si–S correlation is coal fly ash. Mamane and Dzubay (1986) microscopically identified 11% of the particles from one DCL coarse particle sample as fly ash, but unfortunately did not report any such fine particle analysis.

The second major group of highly correlated parameters consists of Zn, Mn, Fe and K, elements associated with industrial and related anthropogenic activities. Arsenic and Pb also have moderate correlations with this group of elements. Although Pb appears with this group, Br does not, indicating a source for Pb in addition to motor vehicles. The wind sector NNW is moderately correlated with Zn and Mn, suggesting Pittsburgh, PA as a possible source area for this elemental group (Fig. 4).

Soil-related elements K, Ca, Sc and Si make up the third major grouping of mutually correlated parameters. Lanthanum is also very likely in this group on the bases of its substantial correlations and modest enrichment factors (Zoller *et al.*, 1974) with respect to these elements. Using the crustal abundances of Mason (1966) the enrichment factors for La are about two relative to K and Ca, and about five relative to Sc and Si. Sodium's highest correlation is with La and its enrichment factors relative to the previous five elements are in the range 0.7–2.

Bromine and Pb are well correlated, as expected, due to their assumed motor vehicle origin. Nitrogen oxides are correlated (weakly) only with these two elements.

The only correlation of V is with the ENE and NNE wind sectors. While this is consistent with the eastern and northeastern U.S. being a region of substantial oil-burning activity, there may be an additional local influence. From the Allegheny Mountain and the Laurel Hill data taken concurrently with the DCL measurements Pierson *et al.* (1989) observed greatly increased V concentrations (10–100 ×) when the wind was from the *southeast* (160° at Allegheny, 135° at Laurel). The same observation was made at Allegheny in 1977 (Pierson *et al.*, 1980). If the back trajectory for the high V case in the DCL set, previously omitted as an outlier, were taken together with Pierson's observations, triangulation defines an approximately 15 km-long region lying between the Allegheny site and Cumberland, MD (Fig. 4). We have not, however, been able to identify a candidate V emission source in this area.

SUMMARY AND CONCLUSIONS

A 1 month intensive field study conducted near Deep Creek Lake in rural western Maryland resulted in a comprehensive high-quality set of fine particle, gaseous and meteorological data. Particulate S in the assumed form of ammonium sulfate constituted 67% of the fine particle mass on average. Fine particle S and mass tracked each other remarkably well over

Table 5. Linear correlation coefficients (×100) for 95 cases*

	SO_2	Se	S	Mass	Zn	Mn	Fe	K	Ca	Sc	Si	La	Na	Br	Pb	V	As	Sb	NO_x	ENE	NNE	NNW	WNW	WSW
SO_2	100																							
Se	68	100																						
S	64	70	100																					
Mass	63	67	99	100																				
Zn	26	49	48	47	100																			
Mn	30	51	54	54	79	100																		
Fe		45	39	37	64	58	100																	
K	26	44	50	51	65	65	63	100																
Ca							35	45	100															
Sc		30				31	45	55	72	100														
Si	45	43	61	66	32	45	47	65	55	61	100													
La	27	31	39	40		35	40	56	47	61	61	100												
Na						29		46		29	35	64	100											
Br							30	33	44	29				100										
Pb					51	47	40	47	39	34	26			80	100									
V																100								
As					50	35	37	30						32	44		100							
Sb		44	29		38	34	29	37		41	31	37	32		28			100						
NO_x														31	32				100					
ENE		−27	−26		−28	−30	−26								−27	40				100				
NNE	−30	−36	−45	−44	−33		−31	−30								40					100			
NNW					49	37						−26			31		36					100		
WNW	32		36	34																	−37	−35	100	
WSW											29	37									−27	−39	−29	100

* Coefficients with absolute values less than 0.26 are omitted.

time ($r = 0.99$). The only other major particulate species (NO_3^-, CEL, CVOL) together can account for no more than 7% of the average fine particle mass, even when including the additional contributions of the cation associated with NO_3^- (probably NH_4^+) and the hydrogen and oxygen associated with volatilizable carbon. This fact, along with the very high correlation coefficient for fine particle S and mass, in an indication of substantial water of hydration associated with particulate SO_4^{2-}.

Sulfur dioxide expressed as S constituted more than half of the total S, indicating that the sampling site was being impacted by local sources.

Selenium, an element expected to come primarily from coal-fired power plants, followed the fine particle S concentration over time fairly well ($r = 0.70$). The ratio of fine particle S to Se was 2800, characteristic of a rural site downwind of coal-burning areas (Tuncel *et al.*, 1985).

Mixed-layer back trajectories were used to calculate wind frequency-normalized concentrations in each of eight wind sectors. Three of the sectors occurred with insignificant frequency and thus were not included in the results. Parameters associated with coal-burning (S, Se, SO_2, fine mass and bsph) were highest for wind trajectories from the west-northwest where the greatest concentration of local and distant coal-burning power plants are located. Normalized concentrations of elements related to anthropogenic activity (Mn, Zn, Br and Pb) were highest for wind trajectories passing through the Pittsburgh metropolitan area. Normalized concentrations of elements related to soil or fly ash (Si, Ca and Fe) were highest in association with wind trajectories passing through less populated areas to the west-southwest. Vanadium was clearly associated with source areas to the northeast, where oil-burning power plants dominate. Parameters which behaved similarly with respect to wind direction were also mutually correlated.

Use of Rahn and Lowenthal regional signatures showed an overwhelming dominance by the Lower Midwest region, and a surprisingly weak impact by the Upper Midwest region.

Any investigator may obtain our data on IBM-PC readable diskettes by sending two 360 kbyte diskettes or one 1.2 Mbyte diskette to one of the authors, Dr Charles W. Lewis.

Although the research described in this report has been funded by the United States Environmental Protection Agency, it has not been subjected to Agency review and, therefore, does not necessarily reflect the views of the Agency, and no official endorsement should be inferred. Mention of commercial products does not constitute endorsement by U.S. EPA.

Acknowledgements—We express our appreciation to Dr William Courtney, Dr William Ellenson, Keith Kronmiller and Dr Charles Tipton for operating the instruments in the field, and Carolyn Owen for preparing the filters. We thank Dr M. Drew Ferrier for logistics support at the DCL site. We are indebted to Dr William Pierson for making available the back-trajectory calculations and for drawing attention to the vanadium phenomenon. We acknowledge the contribution of Dr Bernard Blaustein to the design of the study and the support by the U.S. Department of Energy of key contributors to this project. The Maryland group thanks Ann Sheffield, Dr Ilhan Olmez, Dr Sally Harrison, Ming Han and Janet Joseph for their help. We thank the staff of the National Bureau of Standards nuclear reactor for their help with irradiations. The Maryland portion of the project was supported in part by Sandia National Laboratories under Contract No. 32-0959, the U.S. Environmental Protection Agency under PO No. 6D2560NAET and the State of Maryland Power Plant Research Program under Contract No. PR-88-107-004.

REFERENCES

Countess R. J., Wolff G. T. and Cadle S. H. (1980) The Denver winter aerosol: a comprehensive chemical characterization. *J. Air Pollut. Control Ass.* **30,** 1194–1200.

Courtney W. J., Shaw R. W. and Dzubay T. G. (1982) Precision and accuracy of a β-gauge for aerosol mass determinations. *Envir. Sci. Technol.* **16,** 236–239.

Dzubay T. G., Stevens R. K., Lewis C. W., Hern D. H., Courtney W. J., Tesch J. W. and Mason M. A. (1982) Visibility and aerosol composition in Houston, Texas. *Envir. Sci. Technol.* **16,** 514–525.

Heffter S. L. (1980) Air Resources Laboratory's atmospheric transport and dispersion model. NOAA Technical Memorandum ERL ARL-81, National Oceanic and Atmospheric Administration Air Resources Laboratory, Silver Spring, Maryland, 1980.

Johnson R. L., Shah J. J., Cary R. A. and Huntzicker J. J. (1981) An automated thermal–optical method for the analysis of carbonaceous aerosol. In *Atmospheric Aerosol Source/Air Quality Relationships* (edited by Macias E. S. and Hopke P. K.), ACS Symposium Series **167,** 223–233.

Koutrakis P. and Spengler J. D. (1987) Source apportionment of ambient particles in Steubenville, OH using specific rotation factor analysis. *Atmospheric Environment* **21,** 1511–1519.

Lewis C. W., Baumgardner R. E., Stevens R. K. and Russwurm G. M. (1987) Receptor modeling study of Denver winter haze. *Envir. Sci. Technol.* **20,** 1126–1136.

Loo B. W., Jaklevic J. M. and Goulding F. S. (1976) Dichotomous virtual impactors for large-scale monitoring of airborne particulate matter. In *Fine particles: Aerosol Generation, Measurement, Sampling and Analysis* (edited by Liu B. Y. H.), pp. 311–350. Academic Press, New York.

Lowenthal D. H. and Rahn K. A. (1988) Tests of regional tracers of pollution aerosols. 2. Sensitivity of signatures and apportionments to variations in operating parameters. *Envir. Sci. Technol.* **22,** 420–426.

Mamane Y. and Dzubay T. G. (1986) Characteristics of individual particles at a rural site in the Eastern United States. *J. Air Pollut. Control Ass.* **36,** 906–911.

Mason B. (1966) *Principles of Geochemistry*, third edn. John Wiley, New York.

Parekh P. P. and Husain L. (1982) Ambient sulfate concentrations and wind flow patterns at Whiteface Mountain, New York. *Geophys. Res. Lett.* **9,** 79–82.

Pierson W. R., Brachaczek W. W., Truex T. J., Butler J. W. and Korniski T. J. (1980) Ambient sulfate measurements on Allegheny Mountain and the question of atmospheric sulfate in the northeastern United States. *Ann. N.Y. Acad. Sci.* **338,** 145–173.

Pierson W. R., Brachaczek W. W., Gorse R. A. Jr., Japar S. M., Norbeck J. M. and Keeler G. J. (1987) Acid rain and atmospheric chemistry at Allegheny Mountain. *Envir. Sci. Technol.* **21,** 679–691.

Pierson W. R., Brachaczek W. W., Gorse R. A. Jr., Japar S. M., Norbeck J. M. and Keeler G. J. (1989) Atmospheric

acidity measurements on Allegheny Mountain and the origins of ambient acidity in the northeastern United States. *Atmospheric Environment* **23**, 431–459.

Rahn K. A. and Lowenthal D. H. (1985) Pollution aerosol in the Northeast: Northeastern–Midwestern contributions. *Science* **228**, 275–284.

Samson P. J. (1980) Trajectory analysis of summertime sulfate concentrations in the northeastern United States. *J. appl. Met.* **19**, 1382–1394.

Shah J. J., Watson J. G., Cooper J. A. and Huntzicker J. J. (1984) Aerosol chemical composition and light scattering in Portland, Oregon: the role of carbon. *Atmospheric Environment* **18**, 235–240.

Shaw R. W. Jr., Stevens R. K., Bowermaster J., Tesch J. W. and Tew E. (1982) Measurement of atmospheric nitrate and nitric acid: the denuder difference experiment. *Atmospheric Environment* **16**, 845–853.

Stevens R. K. (1986) Modern methods to measure air pollutants. In *Aerosols: Research, Risk Assessment and Control Strategies* (edited by Lee S. D., Schneider T., Grant L. D. and Verkerk P. J.), pp. 69–95. Lewis Publishers, Chelsea, MI.

Tuncel S. G., Olmez I., Parrington J. R., Gordon G. E. and Stevens R. K. (1985) Composition of fine particle regional sulfate component in Shenandoah Valley. *Envir. Sci. Technol.* **19**, 529–537.

Watson J. G., Cooper J. A. and Huntzicker J. J. (1984) The effective variance weighting for least squares calculations applied to the mass balance receptor model. *Atmospheric Environment* **18**, 1347–1355.

Zoller W. H., Gladney E. S. and Duce R. A. (1974) Atmospheric concentrations and sources of trace elements at the South Pole. *Science* **183**, 198–200.